Research Square

Preprints are preliminary reports that have not undergone peer review.
They should not be considered conclusive, used to inform clinical practice,
or referenced by the media as validated information.

Modelling seasonal patterns, climatic coherence and forecasting future of PPR in Ekiti state, Nigeria

Emmanuel Afolabi BAKARE
emmanuel.bakare@fuoye.edu.ng
Federal University Oye Ekiti
Dolapo A. BAKARE
Federal University Oye Ekiti
Theophilus O. BABALOLA
Federal University Oye Ekiti
Oluwaseun A. Mogbojuri
Adekunle Ajasin University
Ronke Dorcas OLORUNFEMI
University of KwaZulu-Natal
Samuel Abidemi Osikoya
Federal University Oye Ekiti

Research Article

Keywords: Peste des Petits Ruminants (PPR), time-series analysis, continuous wavelet transform, climate–disease relationships, SARIMA, outbreak forecasting, seasonal epidemiology

Posted Date: July 6th, 2026

DOI: https://doi.org/10.21203/rs.3.rs-10129990/v1

License: This work is licensed under a Creative Commons Attribution 4.0 International License.
Read Full License

Additional Declarations: No competing interests reported.

Modelling Seasonal Patterns, Climatic Coherence and Forecasting Future of Peste des Petits Ruminants Outbreaks in Ekiti State, Nigeria

Emmanuel A. Bakare[2,3,*], Dolapo A. Bakare[1,3,*], Theophilus O. Babalola[1], Oluwaseun A. Mogbojuri[2,3,4], Ronke D. Olorunfemi[3,5], and Samuel A. Osikoya[2,3]

[1]Department of Animal Production and health, Federal University Oye - Ekiti, Ekiti State, Nigeria
[2]Department of Mathematics, Federal University Oye - Ekiti, Ekiti State, Nigeria
[3]International Centre for Applied Mathematical Modelling and Data Analytics, Federal University Oye - Ekiti, Nigeria
[4]Department of Mathematical Sciences, Adekunle Ajasin University, Akungba-Akoko, Nigeria
[5]School of Mathematics, Statistics and Computer Science, University of KwaZulu-Natal, Durban, South Africa

Abstract

Background/Aim:
Peste des Petits Ruminants (PPR) is a highly contagious transboundary viral disease posing a severe threat to small ruminant production in Nigeria. Despite its endemic status and significant economic burden in Ekiti State, no study has specifically targeted seasonal pattern identification, climatic coherence analysis, or outbreak forecasting for this region, to he best of our knowledge. This study aimed to characterise the seasonal dynamics and climatic drivers of PPR incidence in Ekiti State, Nigeria, and to generate a 20-month outbreak forecast.

Methods: Monthly PPR case data (January 2015 – September 2025) obtained from the Ekiti State Ministry of Agriculture were analysed alongside NASA POWER climate data. Continuous wavelet transform (CWT), cross-wavelet transform (XWT), and wavelet coherence analyses were applied to identify periodic structures and climate–disease relationships. A Seasonal Autoregressive Integrated Moving Average (SARIMA) model was developed and validated against a 15% hold-out test set, with model selection guided by AIC and performance evaluated using RMSE, MAE, and MAPE.

Results: Wavelet power spectrum analysis revealed a dominant annual cycle in PPR incidence (9–15 month band), strongest during 2015–2019, with a secondary interannual signal at 18–24 months. Cross-wavelet analysis showed significant co-movement between PPR cases and humidity (0.7–0.8 power) and temperature (0.8–0.9 power) within the 8–16 month band. Humidity was found to lead PPR cases by 3–5 months in-phase, while

temperature exhibited an anti-phase relationship, with PPR cases rising during cooler periods. The SARIMA$(3,0,3)(3,1,3)_{12}$ model achieved the best performance (RMSE = 0.818, MAE = 0.680, MAPE = 0.358), forecasting monthly case counts averaging 22–55 through May 2027, with seasonal troughs in January–February and peaks in September–October.

Conclusion: This study elucidates the seasonal dynamics of PPR in Ekiti State, explores its relationship with climatic variability, and forecasts future disease incidence. The findings provide valuable evidence for optimizing the timing of vaccination and surveillance programmes and for supporting data-driven, seasonally targeted PPR control strategies.

Keywords: Peste des Petits Ruminants (PPR); time-series analysis; continuous wavelet transform; climate–disease relationships; SARIMA; outbreak forecasting; seasonal epidemiology.

1 Introduction

Small ruminant production (goats and sheep) is an important component of smallholder agricultural systems in many developing countries, providing income, nutrition and an emergency financial cushion that helps to sustain household livelihoods (ZUMANYE et al., 2025; Aboah et al., 2024). Despite its critical role in smallholder livelihoods, livestock production is severely affected by infectious diseases(ZUMANYE et al., 2025). Peste des petits ruminants (PPR), in particular, poses a serious threat to small ruminants, causing high mortality, significant economic losses and jeopardizing the sustainability of smallholder production systems(ZUMANYE et al., 2025).

Peste des petits ruminants (PPR) is a highly contagious, economically important transboundary viral disease of small ruminants, especially goats and sheep, caused by the small ruminant morbillivirus (SRMV) of the *Paramyxoviridae* family, which is closely related to rinderpest and measles viruses, it is a lymphotropic and epitheliotropic illness that affects the respiratory and digestive systems (Jemberu et al., 2022; Akwongo et al., 2022). In naïve populations, it can cause severe morbidity (80-90%) and mortality (50-80%), limiting small ruminant output internationally (Baron et al., 2016). Virus transmission occurs mainly by direct contact and has limited survival outside the host, the incubation period typically ranges from 3–14 days with acute disease characterized by pyrexia, depression, mucopurulent oculo-nasal discharges, stomatitis, diarrhea, respiratory distress, and occasionally abortion, which may ultimately result in recovery or death (Walle et al., 2024; Woma et al., 2016; Parida et al., 2015).

Evidence suggests that PPR originated in Africa, where it was first identified in Cote d'Ivoire in 1942 and has expanded across the Middle East, Asia and Eastern Europe, threatening nearly 80% of the global sheep and goat population and causing annual losses of USD 2.1 billion(WOAH, 2026a). While sustained transmission has plagued sub-Saharan Africa since the 1990s and active circulation continues across East Africa and Egypt, the burden is particularly severe in Nigeria (Chai et al., 2026; WOAH, 2026b; Esonu et al., 2022). In the Nigerian context, the disease is endemic, with recurrent outbreaks as recent as 2017 that resulted in staggering annual economic losses of approximately ₦4.3 billion ($10.4 million) (Esonu et al., 2022). This widespread impact on small ruminant production has galvanized the international community to target PPR for complete global eradication by 2030 (WOAH, 2026a).

Climatic and environmental factors drive PPR transmission (Chai et al., 2026). Ecological niche modelling identifies the minimum temperature of the coldest month as a key predictor of global PPR distribution, with warmer thresholds favoring outbreak suitability(Agoltsov et al., 2022).

Field evidence from West Africa demonstrates increased outbreaks during the dry harmattan and early dry seasons, when cold, dusty conditions and nutritional stress may heighten host susceptibility (Mantip et al., 2019), while spatiotemporal analyses confirm significant seasonal clustering of outbreaks across rainfall regimes (Alamerew et al., 2025).

Time-series modeling has demonstrated its usefulness for event prediction (Punyapornwithaya et al., 2022). At present, a wide range of time-series methods have been used in several epidemiological studies, resulting in predictive models that can be applied to a variety of data (Punyapornwithaya et al., 2022; Ward et al., 2020). Several studies have employed time-series modeling in veterinary science to identify the seasonal dynamics and forecast of infectious diseases of animals (Ward et al., 2020; Punyapornwithaya et al., 2022). In Ward et al. (2020), the authors applied various methods, including seasonal auto-regressive integrated moving average (SARIMA) and neural network autoregression (NNAR), to study outbreak trends of Foot and Mouth Disease (FMD) outbreaks in cattle farms in Thailand. Using data spanning from January 2010 to December 2020, they provided forecasts and analyzed seasonal patterns, identifying a predominant peak in cases between September and November annually. Their results show that while multiple models performed well, the SARIMA model demonstrated the highest accuracy for out-of-sample validation, highlighting an overall rising trend of FMD episodes in the region.

In India, Zhang et al. (2022) compared the Winters multiplicative model and ARIMA model using outbreak data from 2005–2018 to predict future PPR occurrence. Their findings showed significant seasonality, with outbreaks peaking during cold/dry and wet periods, particularly between January–March and September–December. The forecasts also suggested that PPR outbreaks were likely to persist through 2020 within a 95% confidence interval. A SARIMA model was applied by ZUMANYE et al. (2025) to forecast the vaccination trends of peste des petits ruminants in northern Ghana using data from 2017–2022. The model identified seasonal fluctuations and projected a decline in vaccination coverage by 2024. Several studies have also applied machine learning, spatial analysis and statistical modelling techniques to predict the distribution and transmission dynamics of Peste des petits ruminants in endemic regions, including China and Uganda (Niu et al., 2022; Nkamwesiga et al., 2022).

Wavelet analysis has become an effective method for detecting concealed patterns in epidemiological time series and offering significant insights into the fundamental mechanisms of epidemiological processes (Bakare et al., 2025). Various studies have been carried out in recent decades using wavelet analysis to analyse times-series of infectious disease (Bakare et al., 2025; Su et al., 2020). Bakare et al. (2025) applied wavelet analysis to mpox time series data in Nigeria, revealing a strong annual cycle in transmission most prominent between June 2022 and June 2023, with significant periodicity concentrated in the 12–18 month band. In a study carried out by Hutter et al. (2018), cross wavelet coherence analysis was used to investigate the relationship between ENSO, climatic variables, and cattle rabies outbreaks in Costa Rica, revealing significant coherence between outbreaks and temperature at interannual cycles of 2–6 years.

Despite the extensive forecasting studies aimed at comprehending worldwide PPR patterns, there is a deficiency of study specifically dedicated to predicting PPR outbreaks in Ekiti state, Nigeria to the best of our knowledge. A lack of outbreak prediction may pose some challenges in the formulation of an effective PPR surveillance and control program in Ekiti state, Nigeria. Given the impact of the disease and seasonal patterns, This study therefore aims to identify the seasonal trends and hidden patterns in the outbreak of PPR in Ekiti state Nigeria, and

forecasting the trends and burden of PPR in Ekiti state Nigeria over the next 20 months.

2 Materials and methods

2.1 Study area

The research study was conducted in Ekiti State, located in the southwestern region of Nigeria. Ekiti State is bordered to the north by Kwara State, to the northeast by Kogi State, to the south and southeast by Ondo State, and to the west by Osun State. It lies between longitudes 4°51′ and 5°45′ East of the Greenwich meridian, and latitudes 7°15′ and 8°51′ north of the Equator. The state is primarily an upland zone, rising over 250 meters above sea level, and exhibits a mix of urban, peri-urban, and rural settlements. The state is endemic for Peste des Petits Ruminants (PPR), a highly contagious viral disease affecting sheep and goats, which contributes to significant morbidity and mortality in small ruminant populations.

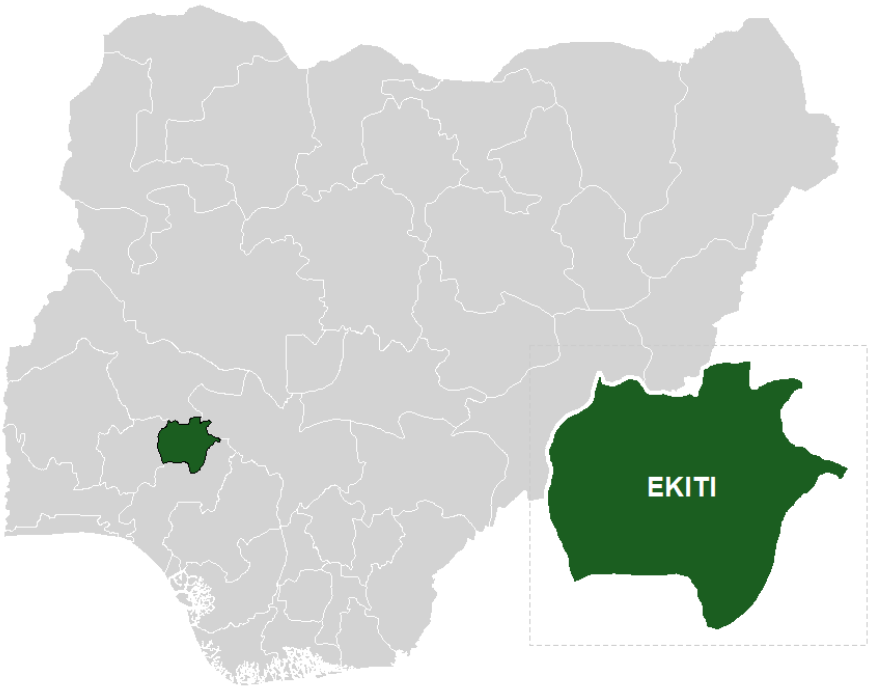


Figure 1: Map of Nigeria showing Ekiti State.

2.2 Data description

2.2.1 *Monthly PPR Cases Data*

This study made use of secondary data obtained from the Department of Veterinary, Livestock and Fisheries Services (VLFS), Ekiti State Ministry of Agriculture and Food Security. The dataset, was extracted from handwritten administrative records of reported and treated cases of Peste des petits ruminants within the state, covering the period from January 2015 to September 2025.

2.2.2 *Monthly Climate Data*

Monthly climatic data comprising temperature (temperture at 2 metres) and relative humidity(relative humidity at 2 meteres) for Ekiti State were obtained from the NASA POWER data access viewer. The dataset was retrieved to correspond with the study period and was used to assess the potential influence of climatic variability on the temporal dynamics of Peste des petits ruminants outbreaks.

2.3 *Wavelet analysis*

Fourier analysis, while a well-established method for decomposing time series into frequency components, has significant limitations: it cannot determine the timing of specific frequencies and is applicable only to stationary time series (Aguiar-Conraria et al., 2008; Bakare et al., 2026; Grenfell et al., 2001). Since most epidemiological time series are non-stationary, this presents a considerable analytical constraint. Wavelet analysis enables the examination of multi-scale, non-stationary time series data, revealing concealed patterns that would otherwise go undetected (Bakare et al., 2025). It stretches into a long wavelet to capture low-frequency structures and compresses into a short wavelet to capture high-frequency features (Aguiar-Conraria et al., 2008), allowing the wavelet transform to decompose a time series using functions that are narrow in time for high-frequency features and wider for analyzing long-term, low-frequency variations (Cazelles et al., 2007). Wavelet analysis reveals hidden patterns in non-stationary time-series data that would otherwise go undiscovered (Bakare et al., 2025).

2.3.1 *The continuous wavelet transform*

A wave, like a sinusoid, is an oscillating function of time or space. In contrast, wavelets are "small waves" with energy concentrated in time, making them useful instruments for analysing transitory, non-stationary, or time-varying phenomena (Burrus et al., 1998; Bakare et al., 2026). The continuous wavelet transform of a time series $x(t)$ with respect to a mother wavelet $\psi(t)$ is given by (Cazelles et al., 2007)

$$W_x(a,s) = \frac{1}{\sqrt{a}} \int_{-\infty}^{\infty} x(t)\, \psi^* \left(\frac{t-s}{a} \right) dt, \tag{1}$$

The wavelet coefficients $W_x(a,\tau)$ represent the contribution of scales a at different time points τ. The wavelet transform (1) can thus be interpreted as a cross-correlation of a time series $x(t)$ with a set of wavelets $\psi\left(\frac{t-\tau}{a}\right)$ at various scales a and time positions τ.

2.3.2 *The wavelet power spectrum*

The wavelet power spectrum shows how the variance (energy) of a time series is distributed across different frequencies and time. At scale f and time τ, the wavelet power spectrum is given by (Cazelles et al., 2008)

$$S_x(f,\tau) = ||W_x(f,\tau)||^2. \tag{2}$$

When all the wavelet coefficients with frequency f are added together with their standard deviation, we get the global wavelet power spectrum, which is also known as the average power spectrum. It is shown by Cazelles et al. (2007).

$$\overline{S}_x(f) = \frac{\sigma_x^2}{T} \int_0^T ||W_x(f,\tau)||^2 \, d\tau, \tag{3}$$

where σ_x^2 and T are the variance and duration of the time series respectively. The global wavelet spectrum offers an impartial and dependable estimation of the true power spectrum of

a time series, generally displaying similar characteristics and structure to the associated Fourier spectrum (Cazelles et al., 2007; Bakare et al., 2026).

2.3.3 *Cross wavelet, wavelet coherency and phase difference*

The frequency correlations between two signals can be obtained by using cross wavelet analysis (CWA) Pienaar (2016). In order to find areas of shared strength, the cross spectrum uses the scale-dependent correlation in the power spectra of independent variables to its advantage (Pienaar, 2016). The term "cross spectrum" is defined as,

$$W_{xy}(u,s) = W_x^*(u,s)W_y(u,s), \tag{4}$$

where $W_x^*(u,s)$ denotes the complex conjugate of $W_x(u,s)$, and x and y represent two independent signals. The phase is provided by the argument of the cross-wavelet $\arg[W_{xy}]$, from which it is possible to derive lead and lag times for each scale (Pienaar, 2016). The phase is calculated as

$$\phi(u,s) = \tan^{-1}\frac{\Im[W_{xy}(u,s)]}{\Re[W_{xy}(u,s)]} \tag{5}$$

where $\mathrm{Im}[W_{xy}(u,s)]$ and $\mathrm{Re}[W_{xy}(u,s)]$ represent the imaginary and real parts of the cross wavelet, respectively.
The instantaneous time-lag between two signals is calculated using the phase angle $\phi(u,s)$ as

$$T_{xy}(u,s) = \frac{\phi_{xy}(u,s)}{2\pi f(u)}. \tag{3.35}$$

The synchronisation of oscillations across a distinct set of wavelengths that define the similarity between the time series is implied by the presence of phase correlation between two signals (Pienaar, 2016). Lead or lag times ranging from $-\pi$ to $+\pi$ for each scale indicate a causal relationship, assuming there is a good basis for it. A useful measure of coherency is called cross wavelet coherency, which provides a normalised covariance modulus with values in the range 0–1. It is defined as the square of the cross spectrum normalised by the individual power spectra (Prokoph and El Bilali, 2008; Pienaar, 2016) as

$$R^2(u,s) = \frac{\left|S\left(W_{xy}(u,s)\right)\right|^2}{S\left(\left|W_x(u,s)\right|^2\right) S\left(\left|W_y(u,s)\right|^2\right)}, \tag{3.36}$$

where S denotes a smoothing operator that operates across both the scale and temporal dimensions. Smoothing is essential; otherwise, all values would converge to 1. The utility of cross wavelet coherency resides in its capacity to demonstrate phase correlation between time series, even in the presence of low-power relationships (Pienaar, 2016).

2.4 *SARIMA model*

In 1976, Box and Jenkin introduced the Autoregressive Integrated Moving Average (ARIMA) method, which has since become one of the most widely used tools for univariate time series modeling. ARIMA is built on three foundational components: the Autoregressive (AR) model, the Moving Average (MA) model, and their combination, the ARMA model (Milenković et al., 2018; Bakare et al., 2026).
The AR model expresses the current value of a time series as a linear function of its past values and current residuals, while the MA model expresses it in terms of current and previous residual series (Rostampour and Masoudi, 2023). The ARMA model integrates both, representing the current value as a linear function of prior observations and residual terms. A key assumption

underlying all three models is stationarity, that is, the time series must have a constant mean and covariance structure over time (Rostampour and Masoudi, 2023).
For non-stationary series, a differencing procedure is first applied to achieve stationarity. This is precisely where ARIMA extends the ARMA framework: by incorporating an integrated differencing step that transforms non-stationary data into a stationary form, making the model suitable for a broader class of real-world time series (Rostampour and Masoudi, 2023). The ARIMA model is expressed as:

$$y_t = C + \phi_1 y_{t-1} + \phi_2 y_{t-2} + \cdots + \phi_n y_{t-n} + \theta_1 \varepsilon_{t-1} + \theta_2 \varepsilon_{t-2} + \cdots + \theta_q \varepsilon_{t-q} + \varepsilon_t. \tag{6}$$

Where C signifies the intercept; ϕ_i $(i = 1, 2, \ldots, p)$ represents the parameters of the autoregressive (AR) component; θ_i $(i = 1, 2, \ldots, q)$ denotes the parameters of the moving average (MA) component; y_t indicates the value of the time series at time t; $y_{t-1}, y_{t-2}, \ldots, y_{t-p}$ denote the preceding values of the series; and ε_t represents the random error or residual term at time t (Bakare et al., 2026).

The SARIMA model is an extension of the ARIMA model specifically designed for univariate time series exhibiting a seasonal component. The model is expressed as ARIMA(p, d, q) $\times$ (P, D, Q)s, where the non-seasonal components are indicated by p, d, and q, representing the autoregressive order, differencing order, and moving average order, respectively (Kaur et al., 2023). The seasonal components are represented as P, D, and Q, indicating the autoregressive (AR) order, differencing order, and moving average (MA) order, respectively, while s signifies the length of the seasonal pattern (Kaur et al., 2023).Mathematically, the SARIMA model is expressed as

$$x_t = \sum_{i=1}^{p} \phi_i x_{t-i} + \sum_{j=1}^{P} \Phi_j x_{t-js} + \varepsilon_t + \sum_{k=1}^{q} \theta_k \varepsilon_{t-k} + \sum_{l=1}^{Q} \Theta_l \varepsilon_{t-ls}, \tag{2}$$

In this context, x_t represents the fully differenced time series, encompassing both non-seasonal and seasonal aspects. The parameters p, d, and q denote the orders of the non-seasonal autoregressive (AR), differencing, and moving average (MA) components, respectively. Similarly, P, D, and Q indicate the orders of the seasonal AR, differencing, and MA components. The variable s signifies the seasonal period. The coefficients ϕ_i and θ_k correspond to the non-seasonal AR and MA components, while Φ_j and Θ_l pertain to the seasonal AR and MA coefficients. Lastly, ε_t represents the white noise error term (Kaur et al., 2023).

3 Results

The wavelet power spectrum of PPR incidence in Ekiti State is presented in (Fig. 2a). The colour code for power ranges from deep blue (low power) to deep red (high power). The cone of influence (COI), which shows the region where edge effects are significant, is described using shaded, semi-transparent white/lighter area that curves down from the top corners. The deep red area between the 9–15 month periodic band indicates a strong annual cycle in PPR reported cases, predominantly between 2015 and 2019 (Fig. 2a). A second, but weak power band is visible around the 18–24 month period, particularly from 2017 to 2022 (Fig. 2a). The annual signal notably weakens after 2019. The global wavelet power spectrum shows a prominent peak around 10–12 months, suggesting a strong annual cycle in PPR incidence in Ekiti State, with a secondary peak around 32–40 months indicating a longer interannual cycle (Fig. 2a).
The wavelet power spectra of temperature and relative humidity in Ekiti State are presented in (Fig. 2c) and (Fig. 2e) respectively. The colour code ranges from deep blue (low power) to deep

red (high power), with the COI shown by the shaded triangular boundary. For both variables, a dominant deep red band around the 9–12 month periodic band throughout the study period indicates a strong and persistent annual cycle in both temperature and relative humidity(Fig. 2c), (Fig. 2e). The global wavelet power spectra confirm this, showing a dominant statistically significant peak around the 9–12 month band exceeding the 0.05 significance threshold for both variables (Fig. 2d) and (Fig. 2f) , suggesting that temperature and relative humidity share a common annual periodicity in Ekiti State.

3.1 *Cross-Wavelet and Coherence Analyses*

3.1.1 *Cross-wavelet analysis of PPR reported cases and humidity*

The cross-wavelet transform (XWT) analysis between humidity and PPR reported cases in Ekiti State revealed statistically significant co-movement power (0.7–0.8) concentrated within the 8–16 month periodicity band, particularly during 2015–2020 and re-emerging in 2022–2025, indicating a strong and recurring seasonal coupling between the two variables (Fig. 3a). The rightward-pointing phase arrows within the significant regions confirm an in-phase relationship, whereby humidity and PPR reported cases rise and fall together, while the phase difference plot further demonstrates that humidity leads PPR reported cases by approximately 2–3 radians (3–5 months) during 2015–2020, before converging toward zero-phase synchrony by 2024–2025, suggesting the lag between humidity peaks and PPR surges has progressively narrowed over the study period (Fig. 3b).

3.1.2 *Cross-wavelet analysis of PPR reported cases and temperature*

The cross-wavelet transform (XWT) analysis between temperature and PPR cases in Ekiti state revealed statistically significant co-movement power reaching 0.8–0.9 within the 8–16 month periodicity band, observed strongly during 2015–2020 and re-emerging in 2022–2025, confirming a robust and persistent seasonal coupling between temperature and PPR incidence (Fig.3c). The rightward-pointing phase arrows within the significant contours indicate an in-phase relationship, meaning temperature and PPR cases co-vary in the same direction. However, the phase difference plot tells a more nuanced story, during 2015–2020, the phase difference stabilizes around -3 radians, indicating that temperature and PPR are anti-phase, whereby PPR reported cases tend to rise as temperature falls, suggesting that cooler seasonal periods drive higher PPR burden (Fig. 3d). Around 2022–2023, the phase difference shifts upward toward $+2$ radians, before dramatically oscillating near $+5$ to -6 radians by 2024–2025, reflecting an increasingly unstable and complex phase relationship in recent years, possibly driven by climate variability or changing disease dynamics.

Table 1: Pearson correlations between PPR reported cases and climate variables in Ekiti

Variable	**r**	**P-value**	**95% CI**
PPR–Humidity	0.1975	0.0248	(0.0256 – 0.3582)
PPR–Temperature	-0.1959	0.0261	(-0.3566 – -0.0238)

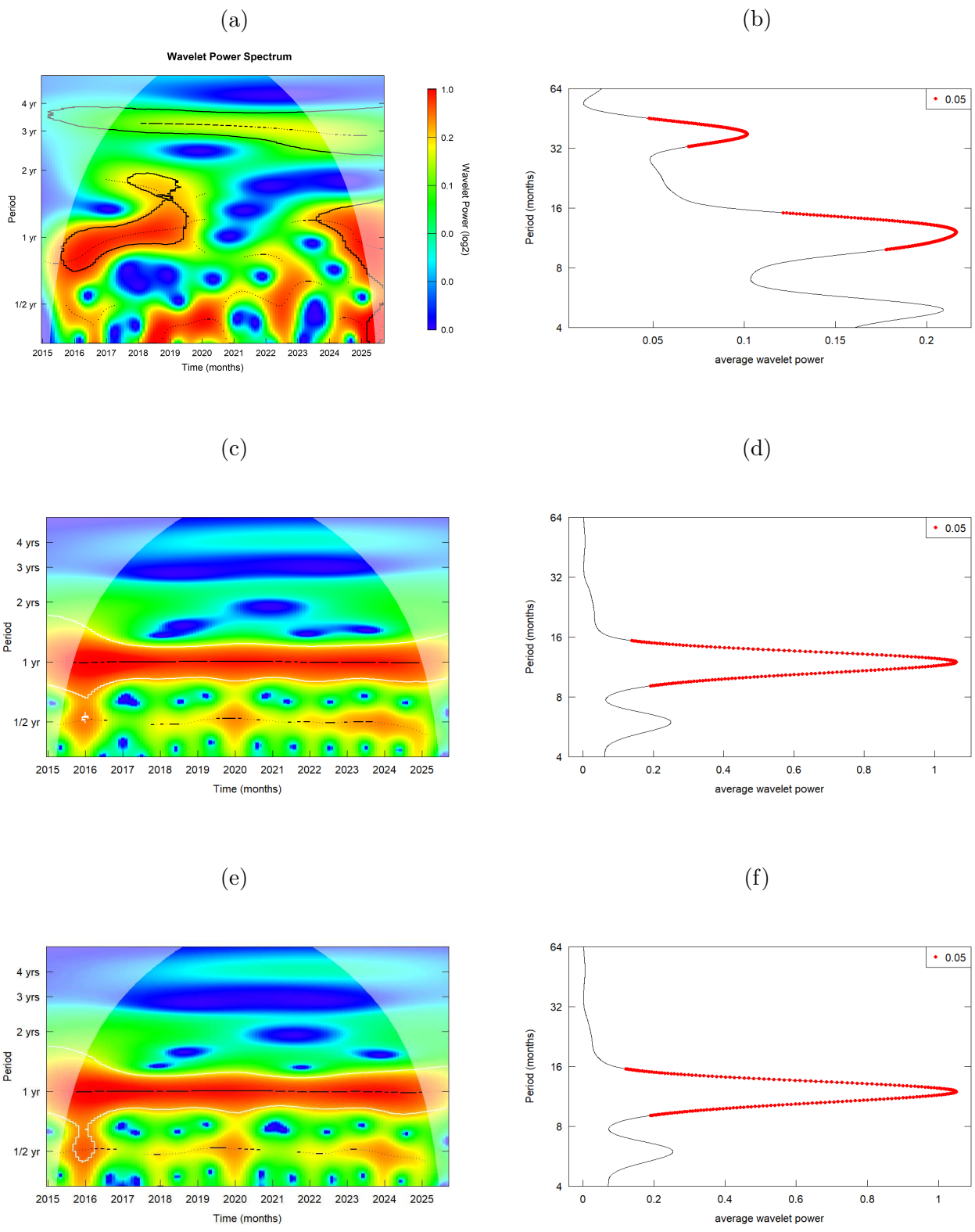


Figure 2: Wavelet power spectra and global wavelet power spectra of PPR cases (a, b), temperature (c, d), and relative humidity (e, f) in Ekiti State, Nigeria (Jan.2015– sept.2025).

3.2 *Forecasting PPR cases*

The time-series analysis started with a description of the data, covering its source, initial quality checks and any preprocessing steps required to ensure suitability for modelling. To reduce heteroscedasticity and improve stationarity, a logarithmic transformation was applied to the

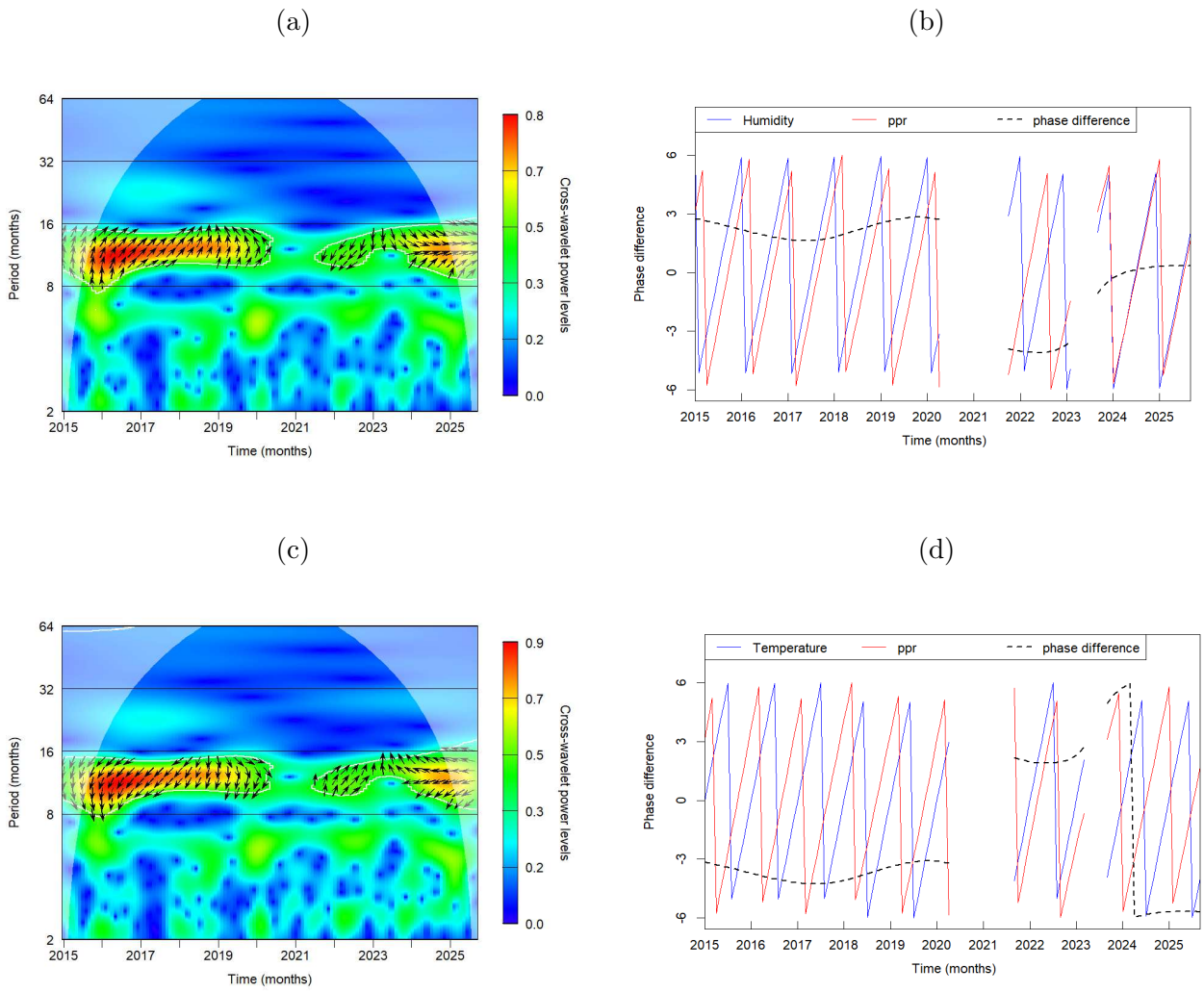


Figure 3: Cross Wavelet and power spectra and global wavelet power spectra of PPR cases (a, b), temperature (c, d), and relative humidity (e, f) in Ekiti State, Nigeria (Jan.2015– sept.2025).

series prior to decomposition (Fig. 4a). The transformed series, along with it's Seasonal-Trend decomposition using Loess (STL) plots, is shown in Fig.4b. The data was then partitioned into a training set (85%, January 2015– February 2024) and a test set (15%, March 2024 – September 2025). The training data were fitted using the auto.arima() function, with candidate models selected based on the Akaike Information Criterion (AIC).

To determine the most effective forecasting model for PPR incidence in Ekiti State, five candidate models were chosen from the auto.arima output and predictive accuracy was assessed. The performance of each model was meticulously validated against the 15% hold-out test data (March 2024 – September 2025) utilising three standard metrics: Mean Absolute Error (MAE), Mean Absolute Percentage Error (MAPE), and Root Mean Square Error (RMSE).A comparative summary of these metrics is presented in Table 2. The SARIMA$(3,0,3)(3,1,3)_{12}$ model was identified as the most robust among the candidates, exhibiting the highest accuracy with an RMSE of 0.8180, MAE of 0.6797, and MAPE of 0.3577.To evaluate the model's reliability, the 129-month dataset was divided into a 110-month training set and a 19-month test set. Fig. 4c demonstrates the correlation between the model's predicted values and the actual test data. Notwithstanding the intricate, multi-scale cycles revealed by the wavelet analysis, the chosen SARIMA model effectively monitors the principal seasonal variations, establishing a statistically robust foundation for forthcoming PPR surveillance in the area.

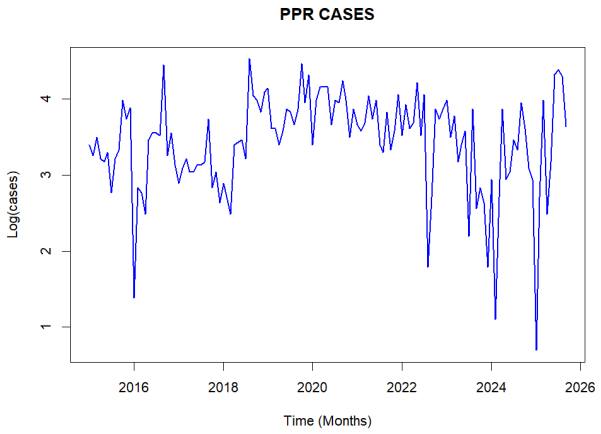
Diagnostic tests were conducted on the residuals of the chosen SARIMA(3,0,3)$(3,1,3)_{12}$ model for Ekiti State to ascertain the model's efficacy in extracting sufficient information from the data. The Ljung-Box test assessed the presence of autocorrelation in the residuals; although the p-value (0.025) indicates residual structure at the 5% significance level, the visual diagnostics offer a more intricate analysis.Fig. 4d presents the diagnostic plots for the model. The time series plot of the residuals indicates a predominantly random distribution around zero, albeit with significant volatility clusters observed in 2022 and late 2024. The ACF plot displays a solitary significant spike at lag 11, while the majority of lags remain within the threshold (blue dashed lines), signifying that most temporal dependencies have been accounted for. The histogram and density plot further validate an approximate normal distribution of the residuals, centred around zero, exhibiting slight skewness and a few outliers in the lower tail. In summary, these diagnostics indicate that although minor irregularities are present, the model effectively represents the principal dynamics of the PPR incidence data.

The selected SARIMA(3,0,3)$(3,1,3)_{12}$ model was used to forecast PPR incidence over a 20-month period, from October 2025 to May 2027. The forecast visualization is illustrated in Fig. 5. The forecast line (blue) is contained within a shaded area representing the 80% and 95% confidence intervals (CI).The 80% confidence interval, denoted by the darker blue-grey region, signifies the range in which the true values are anticipated to reside with an 80% likelihood. The 95% confidence interval, represented by the lighter grey area, offers a wider margin of uncertainty, thereby ensuring a statistically sound framework for future observations. To guarantee the results are practically interpretable, the predicted log-transformed values were reverted to their original scale. Table 3 presents the precise numerical projections for PPR cases in Ekiti State over the designated 20-month period.

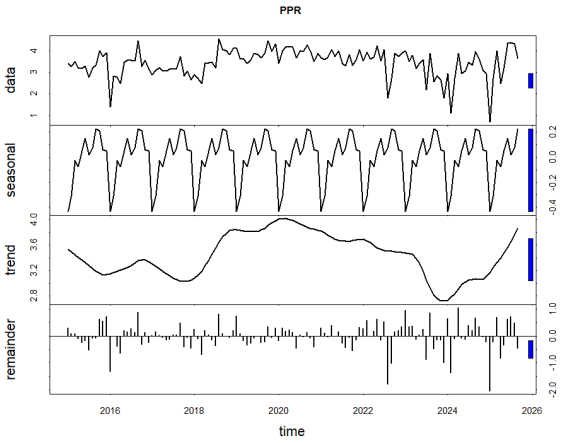
Table 2: Performance comparison of candidate SARIMA models for PPR incidence

Model	**Models** $(p,d,q)\times(P,D,Q)_{12}$	**RMSE**	**MAE**	**MAPE**
Model 1	$(0,1,1)\times(1,0,0)_{12}$	1.0493	0.8541	0.3972
Model 2	$(0,1,1)\times(0,0,1)_{12}$	1.0490	0.8538	0.3972
Model 3	$(0,1,1)\times(1,0,0)_{12}$	1.0493	0.8541	0.3972
Model 4	$(0,1,1)\times(1,0,1)_{12}$	1.0479	0.8583	0.4065
Model 5	$(3,0,3)\times(3,1,3)_{12}$	**0.8180**	**0.6797**	**0.3577**

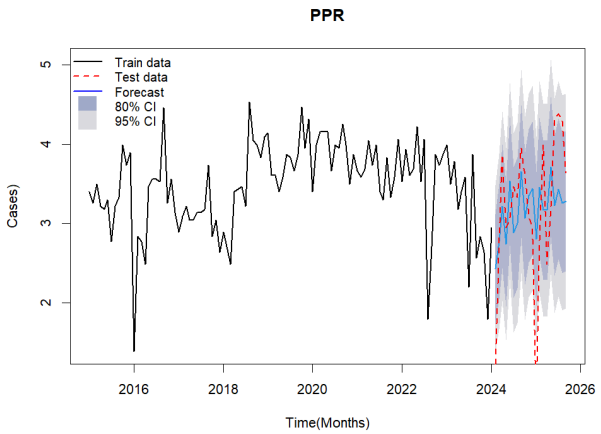
Note: Model 5 shows the lowest error across all metrics and is selected as the best fit for the training data.



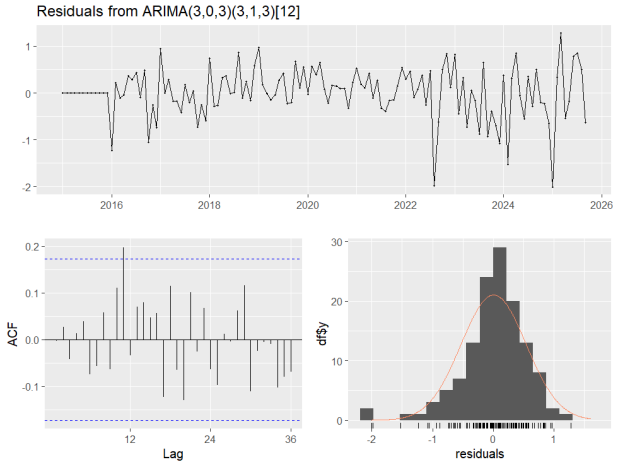
(a) PPR Incidence Data



(b) Time Series Decomposition



(c) 85/15 Train and Test Split



(d) Model Residuals

Figure 4: Time series analysis of PPR incidence in Ekiti State, including data visualization, seasonal decomposition, training/testing partitions, and model diagnostic residuals.

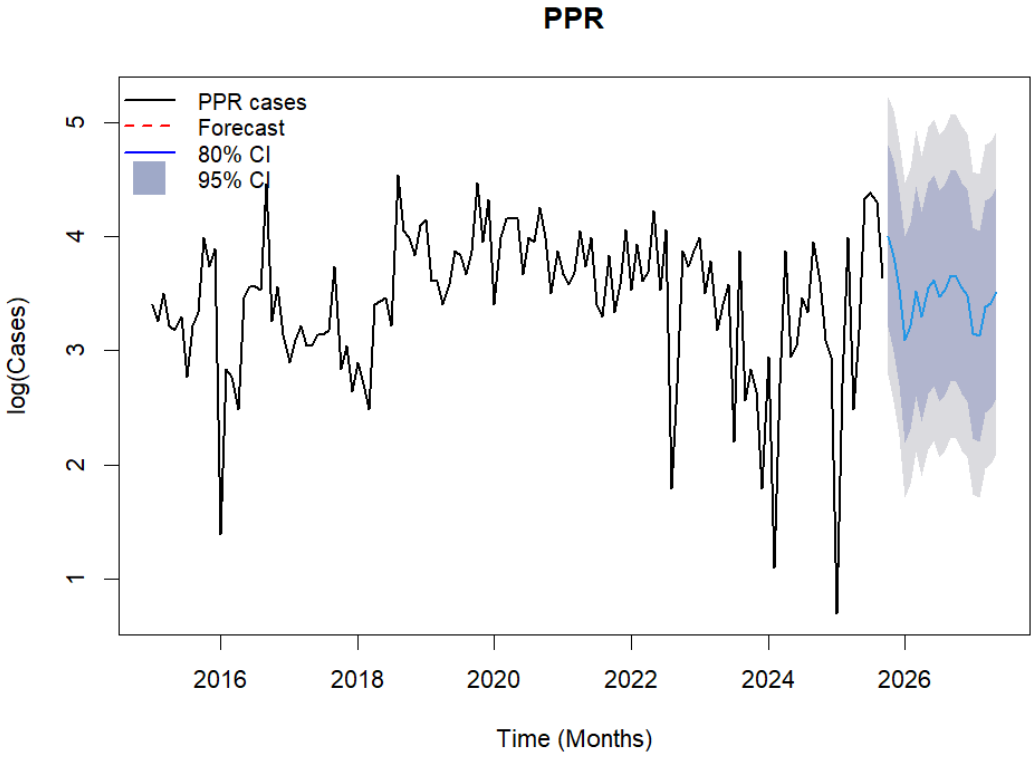


Figure 5: 20-month forecast of PPR incidence in Ekiti State using the SARIMA$(3,0,3)(3,1,3)_{12}$ model. The blue line represents the predicted mean, while the darker and lighter shaded regions indicate the 80% and 95% confidence intervals, respectively.

Table 3: 20-month forecast of PPR incidence in Ekiti State

Time	Forecast	Lower 95% CI	Upper 95% CI	Time	Forecast	Lower 95% CI	Upper 95% CI
Oct 2025	**54.81**	16.28	184.54	Aug 2026	**34.15**	8.33	140.05
Nov 2025	**45.96**	12.90	163.79	Sep 2026	**38.64**	9.42	158.49
Dec 2025	**34.54**	9.49	125.65	Oct 2026	**38.48**	9.34	158.57
Jan 2026	**22.03**	5.54	87.60	Nov 2026	**34.63**	8.40	142.85
Feb 2026	**24.89**	6.23	99.48	Dec 2026	**32.47**	7.87	133.89
Mar 2026	**33.90**	8.31	138.26	Jan 2027	**23.36**	5.68	96.00
Apr 2026	**27.10**	6.64	110.56	Feb 2027	**22.84**	5.56	93.86
May 2026	**34.69**	8.47	142.12	Mar 2027	**29.46**	7.17	121.12
Jun 2026	**37.21**	9.08	152.46	Apr 2027	**30.48**	7.41	125.32
Jul 2026	**32.28**	7.87	132.40	May 2027	**33.31**	8.10	136.95

4 *Discussion*

The wavelet power spectrum of PPR incidence in Ekiti State revealed a dominant and statistically significant annual cycle (9–15 month band), particularly during 2015–2019, indicating that PPR outbreaks follow a strong seasonal pattern (Fig. 2a). This finding is consistent with wavelet-based studies of infectious diseases, where annual periodicity has been identified as a major feature of disease transmission. For example, Bakare et al. (2025) reported a pronounced

annual cycle in mpox incidence in Nigeria and Su et al. (2020) similarly observed that influenza activity in Jinan, China, was characterized by a regular yearly epidemic cycle with distinct seasonal peaks. A secondary significant power cluster was found at 1.5–2 year band, showing inter-annual variability, which is consistent with inter-annual climatic forcing, that has been documented in the epidemiology of tropical diseases. PPR was consistently high during the study period even at sub-annual ($\frac{1}{2}$-year) timescale, indicating a semi-annual periodicity in PPR changes that is not likely to be explained by the environmental or behavioural factors measured here. Results show progressive decreasing in significant power from 2020 to 2023, especially at the annual scale, which could be associated to the disruption caused by COVID-19 pandemic in the disease surveillance, and the return to significant power from 2024 onward, indicating a return to pre-pandemic periodicity patterns. These intrinsic cycles serve as the epidemiological basis for understanding these next climate-PPR coherence analyses.

Cross-wavelet analysis showed significant coherence (0.7–0.8) between humidity and PPR cases within the 8–16 month band, with strong signals during 2015–2020 and 2022–2025. Rightward phase arrows indicate an in-phase relationship, where increases in humidity align with rises in PPR incidence, consistent with dominant wavelet periodicities. This agrees with earlier findings on climate–disease coupling, including lagged weather effects in rabies (Hutter et al., 2018). The persistence of coherence in recent years confirms humidity as a stable driver of PPR seasonality in Ekiti State.
Phase analysis shows a shift over time (Fig.3b). From 2015–2020, phase differences of +2 to +3 radians indicate humidity led PPR cases by 3–5 months, consistent with documented climate–disease lags in similar studies. By 2024–2025, the phase approaches zero, indicating increasing synchrony. This suggests a tightening climate–disease coupling and a reduced lead time, implying that the earlier 3–5 month predictive window is diminishing and that more responsive, climate-integrated surveillance is now required.

XWT analysis between temperature and PPR cases revealed statistically significant co-movement at even higher power magnitudes (0.8–0.9), again concentrated within the 8–16 month band and persisting across 2015–2020 and 2022–2025 (Fig.3c). Despite superficially rightward phase arrows, the phase difference plot exposed a fundamentally distinct relationship from humidity. During 2015–2020, the phase difference stabilized near -3 radians, indicating a near anti-phase relationship in which PPR cases rose as temperatures declined (Fig.3d). This inverse seasonal pattern aligns with the well-established association between harmattan conditions, typically November through February in southwestern Nigeria (Patz et al., 2005). From 2022 onward, the temperature-PPR phase relationship became markedly unstable, oscillating between +2 and -6 radians by 2024–2025. This volatility likely reflects increasing inter-annual climate variability and irregular seasonal temperature patterns, consistent with documented effects of anthropogenic climate change on established disease cycles in tropical regions (McMichael et al., 2006).

The absence of significant XWT power during 2020–2022 in both analyses most plausibly reflects pandemic-related disruptions to routine veterinary health reporting rather than genuine climatological decoupling, an interpretation supported by the rapid re-emergence of significant co-movement power from 2022 onward, a recovery pattern similarly documented for climate-sensitive diseases across sub-Saharan Africa (Food and Agriculture Organization of the United Nations (FAO), 2020; Simegn et al., 2024).

The SARIMA model projected monthly PPR incidence of 33–55 cases over the 20-month forecast horizon (Table 2), with seasonal troughs in January 2026 (22 cases) and January 2027

(23 cases) and peaks in October 2025 (55 cases) and September–October 2026 (39–38 cases). The widening confidence intervals with increasing forecast length reflect the inherent uncertainty of long-term stochastic prediction rather than a loss of seasonal structure (Fig. 5). A similar pattern was reported by Punyapornwithaya et al. (2022) in forecasting foot-and-mouth disease outbreaks, where prediction intervals expanded over time while the models retained their ability to capture recurring seasonal dynamics, underscoring the utility of SARIMA for epidemiological early-warning systems. The persistence of annual peaks and troughs indicates that PPR transmission in Ekiti State remains strongly seasonal rather than random. This finding is consistent with Punyapornwithaya et al. (2022), who reported that foot-and-mouth disease outbreaks in Thailand peaked between September and December, demonstrating that endemic livestock diseases often follow stable seasonal cycles that can be effectively captured by SARIMA models. Similarly, ZUMANYE et al. (2025) employed SARIMA to forecast PPR vaccination trends in northern Ghana, emphasizing that seasonal forecasting provides a valuable tool for planning disease control interventions and resource allocation. Therefore, the projected September–October increase in PPR cases suggests that surveillance and preventive measures should be intensified before this high-risk period to mitigate outbreak occurrence.

The yearly and inter-annual periodicities of the overall incidence of PPR in Ekiti State are found to be strong, with the 8–16 month timescale found to have non-stationary climatic drivers in accordance with the findings of Osikoya et al. (2026) who reported that periodicities of some infectious disease cycles in Nigeria are found to be strong and modulated by non-stationary climatic drivers at 8–16 month timescale. The divergent role of these drivers, with humidity being a positive (synchronous) driver and temperature being a negative (anti-phase) driver, aligns with known observations that the stability of viruses and potential for transmission has been seen to correlate with cooler periods with increased humidity FAO (2015); Dundon et al. (2020). The SARIMA model is able to extract the intrinsic seasonal structure without the need for climatic covariates, while the wavelet results provide a context for the peaks and troughs in the projections as manifestations of the underlying climate-driven structure; both approaches are therefore complementary, with the wavelet results highlighting the climate mechanisms and SARIMA the short-term projections.

This study has contributed to the understanding of the climatic drivers and prediction of PPR in Ekiti State but the results thereof should be interpreted with consideration of certain limitations. There may be underreporting of cases in pastoral and remote communities, which could have contributed to an underestimation of the incidence of disease. Moreover, the SARIMA model itself is only able to capture linear relationships and is therefore not fully able to capture the complex nonlinear nature of PPR transmission or external factors such as vaccination coverage, livestock mobility and animal trade. Such a study should incorporate these factors with a climate-informed forecasting approach like SARIMAX or hybrid epidemiological models to enhance the accuracy of the prediction. The strengthening of the routine monitoring of humidity and temperature in veterinary surveillance system would equally improve early warning capacity and facilitate prompt and targeted PPR control in Ekiti state.

5 *Conclusion*

The study illustrates that the transmission of PPR in Ekiti state has a strong and persistent seasonal structure with obvious dominant annual and inter-annual periodicities that are very much modulated by climatic variability. Humidity was one of the important positive drivers consistently detected by wavelet analysis for PPR dynamics, whereas there was an inverse

and increasingly unstable relationship between disease transmission and temperature. The observed climatic change from 3–5month climatic lead to near synchronous climate–disease dynamics requires that the window of opportunity for intervention is closing, and more responsive monitoring systems are needed. Conversely, SARIMA models captured these seasonal trends and predicted cyclical peaks of transmission in September–October, suggesting that future outbreaks will not be random and will continue to follow seasonal patterns.

The findings from this study are of policy value in the transition from reactive management of outbreaks to anticipatory, climate-informed approach to PPR control in Ekiti State. Ekiti State Ministry of Agriculture and Food Security, and Veterinary authorities, should incorporate meteorological conditions (humidity and temperature) into the routine surveillance and monitoring of animal diseases and should set up early warning systems based on the climate conditions. Immunity-building vaccination campaigns, active surveillance and farmer awareness programs should be planned and executed 2-3 months prior to the expected transmission peak in September-October to maximize immunity of the population and minimize the risk of outbreaks. Improving operational real-time reporting is also crucial to prevent disruptions of surveillance. In conclusion, the integration of climate-informed monitoring and seasonal forecasting offers a feasible approach for optimizing resource allocation, enhancing preparedness, and fostering sustainable PPR control in Ekiti State and across the region in Nigeria, contributing to the overall goal of eradicating PPR.

Ethical considerations

Not applicable

Acknowledgements

The authors sincerely acknowledge the Ekiti State Ministry of Agriculture and Food Security, Nigeria, for providing access to the Peste des Petits Ruminants (PPR) clinical data used in this study. The authors also express their gratitude to Mrs. Adeyemi Temitope, Administrator of the International Centre for Applied Mathematical Modelling and Data Analytics (ICAMMDA), Federal University Oye-Ekiti, for her administrative and logistical support during the course of this research.

CRediT authorship contribution statement

Emmanuel A. Bakare: conceptualization of the study, supervision, interpreted the results and critically reviewed the manuscript. **Dolapo A. Bakare:** Developed the methodology, wrote the manuscript, prepared the figures, performed analysis, interpreted the results, reviewed and edited the manuscripts. **Theophilus O. Babalola:** Supervised, reviewed and edited the manuscripts. **Oluwaseun A. Mogbojuri:** provided technical guidance on epidemiological Modelling and statistical analyses and critically reviewed the manuscript. **Ronke D. Olorunfemi:** Reviewed and edited the manuscripts. **Samuel A. Osikoya:** Reviewed and validated the analytical code, contributed to the verification of the modelling procedures and results and critically reviewed the manuscript.

Consent for publication

Not applicable.

Declaration of competing interest

The authors declare that they have no competing interests or personal relationships that could have appeared to influence the work reported in this paper.

Funding

The authors declare that no external funding was received for this study.

Data availability

The PPR surveillance data used in this study were obtained from the Ekiti State Ministry of Agriculture and Food security and are not publicly available due to institutional restrictions. However, the data are available from the corresponding author upon reasonable request and with permission from the Ekiti State Ministry of Agriculture and Food Security. Climatic data used in this study are publicly available from the NASA POWER database

References

Aboah, J., Campbell, Z. A., Dione, M., Kotchofa, P., Guy, I., Wieland, B., Lo, M., and Rich, K. M. (2024). Economic impact of peste des petits ruminants on small ruminant production in senegal: Gender considerations within a system dynamics modelling approach. *Agricultural Systems*, 217:103928.

Agoltsov, V. A., Podshibyakin, D. V., Padilo, L. P., Chernykh, O. Y., Popova, O. M., Stupina, L. V., and Solotova, N. V. (2022). Analysis of peste des petits ruminants virus spread and the risk of its introduction into the territory of the russian federation. *Veterinary World*, 15(7):1610.

Aguiar-Conraria, L., Azevedo, N., and Soares, M. J. (2008). Using wavelets to decompose the time–frequency effects of monetary policy. *Physica A: Statistical mechanics and its Applications*, 387(12):2863–2878.

Akwongo, C. J., Quan, M., and Byaruhanga, C. (2022). Prevalence, risk factors for exposure, and socio-economic impact of peste des petits ruminants in karenga district, karamoja region, uganda. *Pathogens*, 11(1):54.

Alamerew, E. A., Shite, A., Cherenet, T., and Aklilu, F. (2025). Progress and challenges in peste des petits ruminants control and eradication: a comprehensive review of global strategies and ethiopia's efforts. *Cogent Food & Agriculture*, 11(1).

Bakare, E. A., Mogbojuri, O. A., Bakare, D. A., and Odewusi, O. J. (2026). Exploring the past and forecasting the future of malaria in selected nigerian states: A time series modelling approach using wavelet and sarima. *Plos one*, 21(4):e0337791.

Bakare, E. A., Mogbojuri, O. A., Oniyelu, D. O., Abidemi, A., Daniel, D. O., Olasupo, I. I., Osikoya, S. A., Nwana, A. O., Olorunfemi, R. D., and Olagbami, S. O. (2025). Time series modelling and forecasting of mpox incidence and mortality in nigeria. *BMC Infectious Diseases*, 25(1):794.

Baron, M. D., Diallo, A., Lancelot, R., and Libeau, G. (2016). Peste des petits ruminants virus. *Advances in virus research*, 95:1–42.

Burrus, C. S., Gopinath, R. A., and Guo, H. (1998). *Introduction to Wavelets and Wavelet Transforms: A Primer*. Prentice Hall, Upper Saddle River, NJ. with additional material and programs by Jan E. Odegard and Ivan W. Selesnick.

Cazelles, B., Chavez, M., Berteaux, D., Ménard, F., Vik, J. O., Jenouvrier, S., and Stenseth, N. C. (2008). Wavelet analysis of ecological time series. *Oecologia*, 156:287–304.

Cazelles, B., Chavez, M., Magny, G. C. d., Guégan, J.-F., and Hales, S. (2007). Time-dependent spectral analysis of epidemiological time-series with wavelets. *Journal of the Royal Society Interface*, 4(15):625–636.

Chai, R., Zhang, S., and Joka, D. L. (2026). Analysing spatiotemporal characteristics and estimating the spatial distribution of peste des petits ruminants (ppr) in africa. *Transboundary and Emerging Diseases*, 2026(1):9501187.

Dundon, W. G., Diallo, A., and Cattoli, G. (2020). Peste des petits ruminants in africa: a review of currently available molecular epidemiological data, 2020: Wg dundon et al. *Archives of Virology*, 165(10):2147–2163.

Esonu, D., Armson, B., Babashani, M., Alafiatayo, R., Ekiri, A. B., and Cook, A. J. (2022). Epidemiology of peste des petits ruminants in nigeria: a review. *Frontiers in veterinary science*, 9:898485.

FAO, O. (2015). Global strategy for the control and eradication of ppr. *FAO and OIE*.

Food and Agriculture Organization of the United Nations (FAO) (2020). Guidelines to mitigate the impact of the covid-19 pandemic on livestock production and animal health. Technical report, FAO, Rome, Italy. FAO Animal Production and Health Paper.

Grenfell, B. T., Bjørnstad, O. N., and Kappey, J. (2001). Travelling waves and spatial hierarchies in measles epidemics. *Nature*, 414(6865):716–723.

Hutter, S. E., Käsbohrer, A., González, S. L. F., León, B., Brugger, K., Baldi, M., Mario Romero, L., Gao, Y., and Chaves, L. F. (2018). Assessing changing weather and the el niño southern oscillation impacts on cattle rabies outbreaks and mortality in costa rica (1985–2016). *BMC Veterinary Research*, 14(1):285.

Jemberu, W. T., Knight-Jones, T. J., Gebru, A., Mekonnen, S. A., Yirga, A., Sibhatu, D., and Rushton, J. (2022). Economic impact of a peste des petits ruminants outbreak and vaccination cost in northwest ethiopia. *Transboundary and emerging diseases*, 69(5):e2084–e2092.

Kaur, J., Parmar, K. S., and Singh, S. (2023). Autoregressive models in environmental forecasting time series: a theoretical and application review. *Environmental Science and Pollution Research*, 30(8):19617–19641.

Mantip, S. E., Shamaki, D., and Farougou, S. (2019). Peste des petits ruminants in africa: meta-analysis of the virus isolation in molecular epidemiology studies. *Onderstepoort Journal of Veterinary Research*, 86(1):1–15.

McMichael, A. J., Woodruff, R. E., and Hales, S. (2006). Climate change and human health: present and future risks. *The lancet*, 367(9513):859–869.

Milenković, M., Švadlenka, L., Melichar, V., Bojović, N., and Avramović, Z. (2018). Sarima modelling approach for railway passenger flow forecasting. *Transport*, 33(5):1113–1120.

Niu, B., Liang, R., Zhang, S., Sun, X., Li, F., Qiu, S., Zhang, H., Bao, S., Zhong, J., Li, X., et al. (2022). Spatiotemporal characteristics analysis and potential distribution prediction of peste des petits ruminants (ppr) in china from 2007–2018. *Transboundary and emerging diseases*, 69(5):2747–2763.

Nkamwesiga, J., Korennoy, F., Lumu, P., Nsamba, P., Mwiine, F. N., Roesel, K., Wieland, B., Perez, A., Kiara, H., and Muhanguzi, D. (2022). Spatio-temporal cluster analysis and transmission drivers for peste des petits ruminants in uganda. *Transboundary and emerging diseases*, 69(5):e1642–e1658.

Osikoya, S. A., Bakare, E. A., Akinola, L. O., Oresanya, O., Okoronkwo, C., Eze, N., and Maikore, I. (2026). Wavelet analysis of climate variability and malaria incidence to inform intervention planning in low-and high-burden nigerian states. *medRxiv*, pages 2026–02.

Parida, S., Muniraju, M., Mahapatra, M., Muthuchelvan, D., Buczkowski, H., and Banyard, A. (2015). Peste des petits ruminants. *Veterinary microbiology*, 181(1-2):90–106.

Patz, J. A., Campbell-Lendrum, D., Holloway, T., and Foley, J. A. (2005). Impact of regional climate change on human health. *Nature*, 438(7066):310–317.

Pienaar, M. (2016). On the classification of time series and cross wavelet phase variance.

Prokoph, A. and El Bilali, H. (2008). Cross-wavelet analysis: a tool for detection of relationships between paleoclimate proxy records. *Mathematical geosciences*, 40(5):575–586.

Punyapornwithaya, V., Mishra, P., Sansamur, C., Pfeiffer, D., Arjkumpa, O., Prakotcheo, R., Damrongwatanapokin, T., and Jampachaisri, K. (2022). Time-series analysis for the number of foot and mouth disease outbreak episodes in cattle farms in thailand using data from 2010–2020. *Viruses*, 14(7):1367.

Rostampour, F. and Masoudi, S. (2023). Time series modeling of animal bites. *Journal of Acute Disease*, 12(3):121–128.

Simegn, G. L., Degu, M. Z., Gebeyehu, W. B., Senay, A. B., Krishnamoorthy, J., and Tegenaw, G. S. (2024). Spatiotemporal distribution of climate-sensitive disease incidences in ethiopia: a longitudinal retrospective analysis of malaria, meningitis, cholera, dysentery, leishmaniasis and dengue fever between 2010 and 2022/2023. *BMC public health*, 24(1):697.

Su, W., Liu, T., Geng, X., and Yang, G. (2020). Seasonal pattern of influenza and the association with meteorological factors based on wavelet analysis in jinan city, eastern china, 2013–2016. *PeerJ*, 8:e8626.

Walle, Y., Mugisha, J. Y., Melese, D., and Tessema, H. (2024). Modeling the peste des petits ruminants (ppr) disease transmission dynamics with impacts of vaccination and restocking in small ruminant population in amhara region, ethiopia. *Heliyon*, 10(24).

Ward, M. P., Iglesias, R. M., and Brookes, V. J. (2020). Autoregressive models applied to time-series data in veterinary science. *Frontiers in veterinary science*, 7:604.

WOAH (2026a). Peste des petits ruminants (ppr). Accessed: 29 April 2026.

WOAH (2026b). World animal health information system (wahis): Event management interface. Accessed: 3 March 2026.

Woma, T. Y., Quan, M., Ekong, P. S., Bwala, D. G., Ibu, J. O., Ta'ama, L., Dyek, D. Y., Saleh, L., Shamaki, D., Kalla, D. J., et al. (2016). Serosurvey of peste des petits ruminants virus in small ruminants from different agro-ecological zones of nigeria. *Onderstepoort Journal of Veterinary Research*, 83(1):1–9.

Zhang, S., Liang, R., Yang, Q., Yang, Y., Qiu, S., Zhang, H., Qu, X., Chen, Q., and Niu, B. (2022). Epidemiologic and import risk analysis of peste des petits ruminants between 2010 and 2018 in india. *BMC Veterinary Research*, 18(1):419.

ZUMANYE, E., YENIBEHIT, N., JEBUNI, A., AYAMDOOH, E. N., and ALLEGYE-CUDJOE, E. (2025). Comprehensive trends analysis of peste des petits ruminants (ppr) vaccination in sheep and goats: A study in the northern region of ghana. *Journal of Agriculture, Food, Environment and Animal Sciences*, 6(2):537–558.